

# Is it possible to predict ENSO frequency changes for the coming century?

Fiona Fix<sup>1</sup>, Stefan Alexander Buehler<sup>1</sup>, and Frank Lunkeit<sup>1</sup>

<sup>1</sup>Universität Hamburg

November 23, 2022

## Abstract

El Nino Southern Oscillation (ENSO) is one of the most important climate variabilities on an inter-annual time-scale. We aim to find out whether ENSO frequency will change in a changing climate. We analyse two ensembles of General Circulation Models that participated in the Coupled Model Intercomparison Project Phase 6 (CMIP6) and an initial-conditions ensemble of the MPI-ESM-LR model. We identify the uncertainty caused by natural variability by comparing 120-year time-series of the pre-industrial control and the 1-percent CO<sub>2</sub> simulations for the CMIP6 ensembles. We found that the multi-member mean for all ensembles predicts almost no change in ENSO frequency, but the uncertainties are large, and that most of the inter-member variability can be attributed to natural variability. This means that the impact of inter-model differences might have been overstated in previous studies. This makes it impossible to make reliable predictions of changes in ENSO frequency based on 120-year simulations.



## Abstract

El Niño Southern Oscillation (ENSO) is one of the most important climate variabilities on an inter-annual time-scale. We aim to find out whether ENSO frequency will change in a changing climate. We analyse two ensembles of General Circulation Models that participated in the Coupled Model Intercomparison Project Phase 6 (CMIP6) and an initial-conditions ensemble of the MPI-ESM-LR model. We identify the uncertainty caused by natural variability by comparing 120-year time-series of the pre-industrial control and the 1-percent CO<sub>2</sub> simulations for the CMIP6 ensembles. We found that the multi-member mean for all ensembles predicts almost no change in ENSO frequency, but the uncertainties are large, and that most of the inter-member variability can be attributed to natural variability. This means that the impact of inter-model differences might have been overstated in previous studies. This makes it impossible to make reliable predictions of changes in ENSO frequency based on 120-year simulations.

## Plain Language Summary

El Niño Southern Oscillation (ENSO) is a coupled atmosphere-ocean circulation in the Pacific and of great interest since it impacts weather worldwide. The question how it will change in a changing climate is important to be able to risks due to extreme weather. Global Circulation Models can help assess this question. This study focuses on the question if ENSO frequency will change in a changing climate. We use two ensembles of 43 Global Circulation Models that participated in the Coupled Model Intercomparison Project Phase 6. By comparing the pre-industrial control simulation to a future scenario with increasing CO<sub>2</sub> we can identify the part of the variability caused by different behaviours of the models and the part caused by natural variability. We also use one 68-member ensemble of the MPI-ESM-LR model, because a bigger ensemble might yield statistically more reliable results. We found that on average the models predict only a very small change in ENSO frequency but the uncertainty is big. Because most of this uncertainty can be attributed to the natural variability it can be reduced only marginally. Therefore, it is impossible to make reliable predictions of changes in ENSO frequency based on 120 years of model simulations.

## 1 Introduction

El Niño Southern Oscillation (ENSO) is one of the most important climate variabilities on an inter-annual time-scale. Due to teleconnections it impacts weather conditions worldwide and can lead to extreme weather events. To reduce the social, economic and environmental risk of these events, accurate forecasting is required. Therefore, understanding and predicting ENSO mechanisms is a central question of current research. In particular, the question of how ENSO will react to global warming is of great interest. Global warming could have different effects on the equatorial Pacific and therefore on ENSO. ENSO frequency can be affected by the strength and depth of the equatorial thermocline, the meridional and zonal sea surface temperature (SST) gradients as well as the strength of the trade winds (Yang et al., 2005; Deng et al., 2010). How these (and other) mechanisms work together and which one(s) will predominate, defines how ENSO will react in future and has yet to be investigated. If and how ENSO behaviour will change under a changing climate has been studied intensely in the past years.

Some studies found an increase in ENSO frequency in the models they examined (Timmermann et al., 1999; Collins, 2000a). Collins (2000a) for example studied ENSO frequency with the second Hadley Centre coupled climate model (HadCM2). The HadCM2 is a coupled climate model which, according to Collins (2000a), represents present day ENSO conditions (amplitude and frequency) well. When running different climate change scenarios he finds that there are only small changes until a quadrupling of CO<sub>2</sub>, when the frequency doubles. On the other hand Yang et al. (2005) investigated ENSO in the

59 Fast Ocean-Atmosphere Model and find that a reduction of ENSO frequency is very likely  
60 as a result of warming climate. Yet other studies argue that ENSO frequency does not  
61 react to global warming at all (e.g. Timmermann, 2001; Zelle et al., 2005). Also, Collins  
62 (2000b) follows up on his earlier study and finds that in the third Hadley Centre cou-  
63 pled climate model (HadCM3) there is no change to ENSO frequency under different cli-  
64 mate change scenarios. Both Zelle et al. (2005) and Collins (2000b) emphasise the ef-  
65 fect that model specifics can have on the sensitivity of ENSO to climate change. There-  
66 fore, to increase the robustness multi-model ensembles have been used in many later stud-  
67 ies. In a study by Merryfield (2006) 12 out of 15 models (prepared for IPCC AR4) agreed  
68 on a decrease in ENSO period. Cai et al. (2014); Cai, Santoso, et al. (2015) and Cai, Wang,  
69 et al. (2015) analysed models participating in the Coupled Model Intercomparison Project,  
70 Phases 3 and 5. They conclude, that there is a high inter model agreement, that extreme  
71 El Niño/ La Niña events become more frequent in a warming climate. Wang et al. (2017)  
72 also use 13 models participating in Coupled Model Intercomparison Project Phase 5 (CMIP5)  
73 and come to the same conclusion. But, many studies that have investigated multi-model  
74 ensembles come to the conclusion that the predictions of ENSO frequency are strongly  
75 model dependent. Studies by Guilyardi (2006), Deng et al. (2010), Xu et al. (2017) and  
76 Chen et al. (2017) suggest that the model consensus is very small on the topic of how  
77 ENSO frequency will change in a changing climate.

78 Chen et al. (2017) mention that the difficulty in predicting ENSO properties is not  
79 only the inter-model spread but also the significant natural variability and Zheng et al.  
80 (2018) support this hypothesis in a study about ENSO amplitude. A similar study by  
81 Maher et al. (2018) shows that (depending on the warming scenario) up to 90% of the  
82 variability of ENSO amplitude can be attributed to internal variability. In this study we  
83 want to quantify the aspect of natural variability of ENSO frequency. Climate forecasts  
84 can be improved by using multi-model ensembles (Xu et al., 2017) instead of single sim-  
85 ulations because parametrisation errors of individual models are expected to be averaged  
86 out. The uncertainty due to differences in the model realisation is reducible but it is not  
87 the only uncertainty in such ensembles. The chaotic nature of the climate system will  
88 cause an internal variability which remains irreducible. We want to identify the signal  
89 caused by this internal climate variability. Therefore we make use of the multi-model en-  
90 semble that is part of the Coupled Model Intercomparison Project Phase 6 (CMIP6).  
91 We compare the simulation with increased CO<sub>2</sub> to the pre-industrial control simulation.  
92 By doing so we can estimate how much of the variability is caused by the different model  
93 responses to the forcing and how much is due to internal variability.

94 Additional to the multi-model ensemble we analyse a bigger ensemble resulting from  
95 running the MPI-ESM-LR model with perturbed initial conditions, to increase the sta-  
96 tistical confidence of our results. As suggested by Maher et al. (2018), the use of large  
97 single-model ensembles can give important insight into changes in ENSO properties.

## 98 2 Data

99 In this work we first make use of two multi-model ensembles of CMIP6, which con-  
100 sist of 43 members (a list with detailed information can be found in table 1). We com-  
101 pare the simulations for the 1 percent CO<sub>2</sub> (1pct CO2) experiment to the pre-industrial  
102 Control (piControl) simulations. In the piControl experiment 1850 is used as a reference  
103 year and the simulations are run for at least 500 years (Eyring et al., 2016). The 1pct  
104 CO2 simulation is initialised from the control run. A 150-year period is simulated dur-  
105 ing which the CO<sub>2</sub> concentration is continuously increased by 1% per year. This results  
106 in a doubling of CO<sub>2</sub> after 70 and a quadrupling after 140 years, respectively (Giorgetta  
107 et al., 2013). To make the two ensembles comparable we only use the last 150 years of  
108 the piControl run. For the IPSL model apparently files were added at different times.  
109 Because the files' meta-data implied that the later simulations might not actually be from  
110 the same model version and the first simulation is already 500 years long, we decided to

**Table 1.** List of the 43 CMIP6 models used in this study.

No.	Model	Variant	Version	1pct <sub>Control</sub> <sup>pi</sup>	Institute	Resolution <sup>a</sup> ocean, latxlon	Reference
1	ACCESS-CSM2	rlilp1f1	v20191109	x	CSIRO	300x360	Dix et al. (2019)
2	ACCESS-ESM1-5	rlilp1f1	v201911115	x	CSIRO	300x360	Ziehn et al. (2019)
3	AWI-CM-1-1-MR	rlilp1f1	v20181218	x	AWI	83030 <sup>c</sup>	Semmler et al. (2018)
4	BCC-CSM2-MR	rlilp1f1	v20181015	x	BCC	232x360	Xin et al. (2018)
5	BCC-ESM1	rlilp1f1	v20190611	x	BCC	232x360	Zhang et al. (2018)
6	CAMS-CSM1-0	rlilp1f1	v20190708 <sup>b</sup>	x	CAMS	200x360	Rong (2019)
7	CESM-FV2	rlilp1f1	v20190729 <sup>b</sup>	x	NCAR	384x320	Danabasoglu (2019a)
8	CESM-WACCM-FV2	rlilp1f1	v20200310 <sup>b</sup>	x	NCAR	384x320	Danabasoglu (2019c)
9	CESM2-WACCM	rlilp1f1	v20191120 <sup>b</sup>	x	NCAR	384x320	Danabasoglu (2019d)
10	CESM2	rlilp1f1	v20200226 <sup>b</sup>	x	NCAR	384x320	Danabasoglu (2019b)
11	CIesm	rlilp1f1	v20191120 <sup>b</sup>	x	NCAR	384x320	Danabasoglu (2019b)
12	CNRM-CM6-1-HR	rlilp1f2	v20190320 <sup>b</sup>	x	THU	384x320	Huang (2019)
13	CNRM-CM6-1	rlilp1f2	v20200220 <sup>b</sup>	x	CNRM-CERFACS	1050x1442	Voltaire (2019)
14	CNRM-ESM2-1	rlilp1f2	v20180626 <sup>b</sup>	x	CNRM-CERFACS	294x362	Voltaire (2018)
15	CanESM5	rlilp1f1	v20180814 <sup>b</sup>	x	CNRM-CERFACS	294x362	Seferian (2018)
16	CanESM5	rlilp2f1	v20181115 <sup>b</sup>	x	CCCma	291x360	Swart et al. (2019)
17	E3SM-1-0	rlilp1f1	v20190429	x	CCCma	291x360	Swart et al. (2019)
18	EC-Earth3	r3ilp1f1	v20191008	x	E3SM-Project	180x360	Bader et al. (2019)
19	FIO-ESM-2-0	r2ilp1f1	v20200129 <sup>b</sup>	x	EC-Earth Consortium	292x362	EC-Earth Consortium (2019)
20	GFDL-CM4	rlilp1f1	v20200420 <sup>b</sup>	x	FIO-QLNM	384x320	Song et al. (2019)
21	GISS-E2-1-G	r102ilp1f1	v20200306	x	NOAA-GFDL	1080x1440	Guo et al. (2018)
22	GISS-E2-1-G	rlilp1f1	v20191012	x	NASA-GISS	90x144	NASA/GISS (2018a)
23	GISS-E2-1-G	rlilp5f1	v20180701	x	NASA-GISS	90x144	NASA/GISS (2018a)
24	GISS-E2-1-H	rlilp1f1	v20190201	x	NASA-GISS	90x144	NASA/GISS (2018a)
25	GISS-E2-2-G	rlilp1f1	v20190815	x	NASA-GISS	90x144	NASA/GISS (2018b)
26	HadGEM3-GC31-LL	rlilp1f3	v20190824	x	NASA-GISS	90x144	NASA/GISS (2018b)
27	INM-CM4-8	rlilp1f1	v20190620 <sup>b</sup>	x	MOHC	330x360	Ridley et al. (2018)
28	INM-CM5-0	rlilp1f1	v20190628 <sup>b</sup>	x	INM	180x360	Volodin et al. (2019a)
29	IPSL-CM6A-LR	rlilp1f1	v20190530	x	INM	180x360	Volodin et al. (2019b)
30	MCM-UA-1-0	rlilp1f1	v20200226	x	IPSL	332x362	Boucher et al. (2018)
31	MIROC-ES2L	rlilp1f2	v20190619	x	UA	80x192	Stouffer (2019)
32	MIROC6	rlilp1f1	v20190731	x	MIROC	256x360	Hajima et al. (2019)
33	MPI-ESM1-2-HAM	rlilp1f1	v20190823	x	MIROC	256x360	Tatebe and Watanabe (2018)
34	MPI-ESM1-2-HR	rlilp1f1	v20181212	x	HAMMOZ-Consortium	220x256	Neubauer et al. (2019)
35	MPI-ESM1-2-LR	rlilp1f1	v20190628	x	MPI-M	404x802	Jungclaus et al. (2019)
36	MRI-ESM2-0	rlilp1f1	v20190710	x	MPI-M	220x256	Wieners et al. (2019)
37	MRI-ESM2-0	rlilp1f1	v20190710	x	MRI	363x360	Yukimoto et al. (2019)
38	NESM3	rlilp1f1	v20200303 <sup>b</sup>	x	MRI	363x360	Yukimoto et al. (2019)
39	NorCPM1	rlilp1f1	v20200222 <sup>b</sup>	x	NUIST	292x362	Cao and Wang (2019)
40	NorESM2-LM	rlilp1f1	v20190703	x	NCC	384x320	Bethke et al. (2019)
41	NorESM2-MM	rlilp1f1	v20190704	x	NCC	385x360	Seland et al. (2019)
42	SAM0-UNICON	rlilp1f1	v20190914	x	NCC	385x360	Bentsen et al. (2019)
43	UKESM1-0-LL	rlilp1f2	v20210118 <sup>b</sup>	x	SNU	384x320	Park and Shin (2019)
			v20191108	x	MOHC	330x360	Tang et al. (2019)
			v20190323	x			
			v20190910	x			
			v20190701	x			
			v20200828	x			

<sup>a</sup> Some files have different resolution information in the meta-data .

We use the resolution that can be determined from the size of the variable-array

<sup>b</sup> For these files the creation date precedes the date according to the version number.

We nevertheless assume that the version number date is correct.

<sup>c</sup> Irregular grid, number of grid points

111 use the last 150 years of this first simulation instead of the later ones. The ensembles  
 112 will be referred to as 1pct- and Control-ensemble, respectively.

113 Another ensemble used in this study is an initial-conditions ensemble. The MPI-  
 114 ESM-LR model has been run for the 1pctCO2 experiment with slightly different initial  
 115 conditions which results in a 68-member ensemble (Plesca et al., 2018; Giorgetta et al.,  
 116 2013; Stevens et al., 2013). This ensemble will from now on be referred to as MPI-ensemble.  
 117 It should be mentioned that this ensemble is older than the CMIP6 ones, since it was  
 118 run for the CMIP5. The reason for using an older ensemble for this work was the avail-  
 119 ability of this dataset.

### 120 3 Methods

121 There are many indices to measure ENSO activity, which all have their advantages  
 122 and disadvantages. Depending on the available data and the question posed, different  
 123 indices prove to be helpful. In this work we make use of an index based on the first em-  
 124 pirical orthogonal function (EOF) of SST data from the tropical Pacific (120°E-60°W,  
 125 30°N-30°S). The pattern of the first EOF explains most of the variability in the tropi-  
 126 cal Pacific, particularly in the Nino3.4 region (Dommenget et al., 2013). Therefore, the  
 127 principle component (PC) of the first EOF can be used as an ENSO-index (a very simi-  
 128 lar approach was used in other studies (e.g. Merryfield, 2006; Berner et al., 2020)). In  
 129 fact, it can be shown that this index is highly correlated with the Ocean Nino Index (ONI)  
 130 defined by NOAA Climate Prediction Center, National Weather Service (2020a) (Berner  
 131 et al., 2020; Penland & Sardeshmukh, 1995). This means that they indeed describe the  
 132 same ENSO variations. We calculated the correlation between these two indices for the  
 133 43-member ensemble of the CMIP6 piControl experiment and obtained a mean value of  
 134 0.971 (min: 0.883, max: 0.991).

135 In order to calculate this index the climate trend and annual cycle have to be elim-  
 136 inated. This is done as described by NOAA Climate Prediction Center, National Weather  
 137 Service (2020a) for the ONI. Anomalies are calculated for each grid-point with respect  
 138 to a centred base-period. This base-period is updated every 5 years to account for the  
 139 warming trend in the region. The base-period corresponding to the years  $x$  to  $x+5$  is the  
 140 period  $x-15$  to  $x+15$  (NOAA Climate Prediction Center, National Weather Service, 2020b).  
 141 Subsequently, the anomalies are smoothed by a 3-month-running mean. From these smoothed  
 142 anomalies EOFs can be calculated, which also yields the time series of the PCs. The first  
 143 PC is used as the ENSO-index in this study and will be referred to as the PC-index. The  
 144 base-period-method creates artificial trends at the beginning and end of a dataset, be-  
 145 cause for the first and last 15 years there is no centred base-period available. Therefore,  
 146 the first base-period has to be used for the first 20 years and the last base-period for the  
 147 last 20 years. This creates an unwanted effect, which can't be corrected. Therefore the  
 148 first and last 15 years of data can not be correctly evaluated and will not be taken into  
 149 account for further analysis. We therefore effectively analyse time series with a length  
 150 of 120 years.

151 According to the NOAA Climate Prediction Center, National Weather Service (2020a)  
 152 conditions are considered "El Niño-like" when the ONI exceeds +0.5 K and "La Niña-  
 153 like" when the index goes below -0.5 K. Whenever conditions are met for 5 consecutive  
 154 months, it is called an "El Niño event" or a "La Niña event". We use the same defini-  
 155 tion for the PC-index as well.

156 Similarly to Deng et al. (2010) we count El Niño and La Niña events to estimate  
 157 changes in ENSO frequency. In this study we use a 30-year moving window. The num-  
 158 ber of months within a 30-year period that were "El Niño-" or "La Niña-like" were counted  
 159 as well as the number of actual El Niño or La Niña events within this period. This re-  
 160 sults in a time series of occurrences, of which a linear regression can be calculated. The  
 161 slope of this regression line defines the linear trend in the amount of "El Niño-" and "La  
 162 Niña-like" months and -events. It provides insight into how the number of El Niño/La  
 163 Niña events will increase or decrease over the years. We have computed the linear trend

**Table 2.** Means and standard deviations  $\sigma$  of predicted changes in occurrences of El Niño (EN) and La Niña (LN) events and "EN/LN-like" conditions for all three ensembles<sup>a</sup>.

ensemble	EN		LN		"EN-like"		"LN-like"	
	mean	$\sigma$	mean	$\sigma$	mean	$\sigma$	mean	$\sigma$
1pct	$0.038 \pm 0.038$	0.2506	$0.108 \pm 0.030$	0.1987	$0.094 \pm 0.441$	2.8919	$0.622 \pm 0.444$	2.9101
Control	$-0.040 \pm 0.032$	0.2085	$0.022 \pm 0.040$	0.2615	$-0.290 \pm 0.386$	2.5319	$0.179 \pm 0.412$	2.7047
MPI	$0.070 \pm 0.030$	0.2514	$0.020 \pm 0.029$	0.2364	$-0.169 \pm 0.374$	3.0849	$-0.320 \pm 0.390$	3.2138

<sup>a</sup>All numbers are unitless, they represent changes in occurrences during one decade.

164 for every member of each of the three ensembles. For convenience, the gradient in months<sup>-1</sup>  
 165 can be converted into a more intuitive measure for the change in ENSO frequency by  
 166 multiplying it by 120 months, which then gives the change in the number of occurrences  
 167 during a decade.

## 168 4 Results

169 Figures 1 and 2 show the linear trend of El Niño and La Niña -events and -like months.  
 170 On average the 1pct-ensemble predicts an increase of  $0.038 \pm 0.038$  El Niño events and  
 171 an increase of  $0.108 \pm 0.030$  La Niña events per decade (the  $\pm$  values are the standard  
 172 errors,  $\sigma/\sqrt{N}$ ). The standard deviations ( $\sigma$ ) are 0.2506 and 0.1987 events per decade  
 173 for El Niño and La Niña events, respectively. Hence, the inter-model spread appears to  
 174 be larger than the mean change itself, which makes it difficult to detect changes in ENSO  
 175 frequency (see Tab. 2).

176 An interesting question is whether this uncertainty can be reduced at all. There-  
 177 fore we compare the 1pct-ensemble to the Control-ensemble. It can be expected that the  
 178 1pct-ensemble contains uncertainties ( $\sigma_{1pct}$ ) due to the different reactions of the differ-  
 179 ent models to the forcing ( $\sigma_{ModelDiff}$ ) as well as uncertainties due to the natural variabil-  
 180 ity ( $\sigma_{NaturalVariability}$ ). Under the assumption that the errors are uncorrelated this re-  
 181 sults in

$$182 \quad \sigma_{1pct}^2 = \sigma_{ModelDiff}^2 + \sigma_{NaturalVariability}^2 \quad (1)$$

183 Therefore its standard deviation should be greater than the standard deviation of  
 184 the Control-ensemble, which only contains the uncertainty due to natural variability:

$$185 \quad \sigma_{Control}^2 = \sigma_{NaturalVariability}^2 \quad (2)$$

186 Still under the assumption of uncorrelated errors, the difference in the variances  
 187  $\sigma^2$  of the two ensembles should be a measure for the uncertainty caused by model dif-  
 188 ferences, ie.

$$189 \quad \sigma_{ModelDiff}^2 = \sigma_{1pct}^2 - \sigma_{Control}^2 \quad (3)$$

190 This uncertainty can be reduced, while the rest, the natural variability, will remain.

191 For El Niño events the standard deviation due to model differences is therefore 0.1369  
 192 events per decade, which is one order of magnitude less than the standard deviation due  
 193 to natural variability. For La Niña events the difference in variances is even negative with  
 194  $-0.0281$ .

195 This means that the biggest part of the uncertainty in the 1pct-ensemble predic-  
 196 tion stems from the natural variability and is therefore irreducible, since the real world

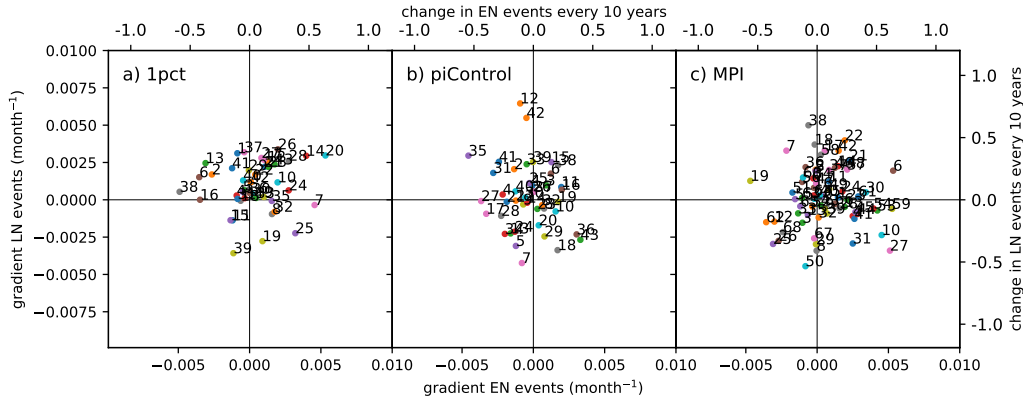


**Figure 1.** Linear Trend in El Niño/La Niña events for each member of the three ensembles: a) the 1pct-ensemble, b) the Control-ensemble, c) the MPI-ensemble. Values towards the top of the plot indicate increasing number of La Niña (LN) events, values toward the right of the plot indicate an increasing number of El Niño (EN) events. Numbers in panels a) and b) correspond to models as in table 1.

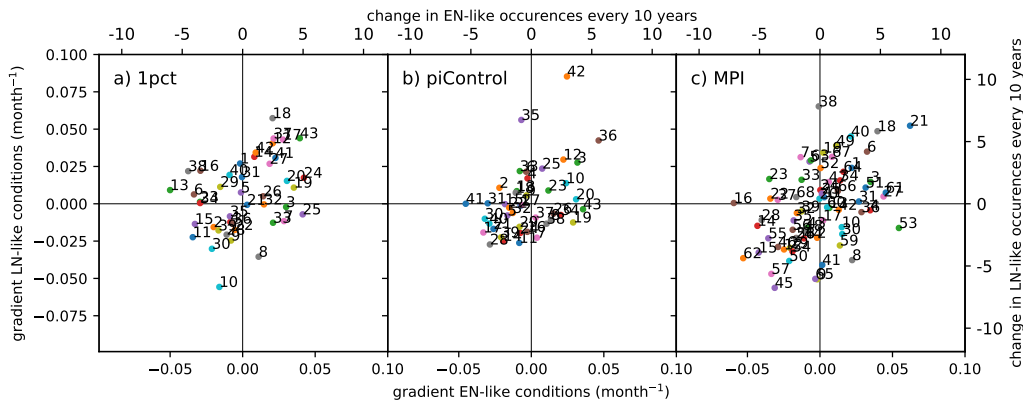


**Figure 2.** Same as figure 1 but for "El Niño-" and "La Niña-like" conditions.

197 will evolve like one ensemble member, not like the ensemble mean. Since the uncertainty  
 198 is in the range of the predicted mean changes or even exceeds them, no reliable forecast  
 199 can be made on the time-scale of 120 years. The result is qualitatively the same for the  
 200 "El Niño-" and "La Niña-like" conditions (see Tab. 2 and Fig. 2)

201 A statistically more reliable result might be achieved by analysing a bigger ensemble.  
 202 Therefore we conducted the same analysis for the MPI-ensemble, which consists of  
 203 68 members. The MPI-ESM-LR model was run with perturbed initial conditions for the  
 204 1pct CO<sub>2</sub> experiment in CMIP5. Since it is an initial-conditions ensemble it only con-  
 205 tains the uncertainty due to natural variability. For the change in El Niño events the big-  
 206 ger ensemble predicts a change of  $0.069 \pm 0.030$  events per decade. The uncertainty seems  
 207 to be slightly less compared to the earlier analysis. But for the La Niña events and the  
 208 "El Niño-" and "La Niña-like" conditions the uncertainty is of the same order of mag-  
 209 nitude or bigger than the expected change itself again. This supports the assumption  
 210 that a reliable prediction of ENSO-frequency on a time-scale of 120 years cannot be made.

## 5 Discussion and Conclusions

The multi-model mean frequency change of El Niño and La Niña events is less than  $\pm 0.2$  events per decade in all three ensembles and in all cases the uncertainties are large. Our analysis of the two CMIP6 ensembles showed that the natural variability dominates the results. This suggests that the stronger trends found in individual models like in the studies by Timmermann et al. (1999) or Yang et al. (2005) may be mostly due to natural variability. Also the results from Timmermann (2001) and Zelle et al. (2005) who found no trend in the respective models therefore have to be treated carefully. In contrast to the studies by Merryfield (2006), Cai et al. (2014), Cai, Wang, et al. (2015), Cai, Santoso, et al. (2015) and Wang et al. (2017) we could not find an inter-model consensus on a significant trend in ENSO frequency in the ensembles. It should be mentioned though, that we did not distinguish between normal and extreme El Niño and La Niña events like some of the mentioned authors did.

Zelle et al. (2005) and Collins (2000b) suggested that prediction of ENSO frequency is strongly model dependent and the studies by Guilyardi (2006), Deng et al. (2010), Xu et al. (2017) and Chen et al. (2017) indeed found a poor inter-model consensus. Our study implies though that it is actually not the model differences that are responsible for the biggest part of the inter-model spread but rather the natural variability. This does not mean that model differences do not play a role, only that their importance relative to natural variability likely has been overstated. We therefore complement the findings of Chen et al. (2017), who found that for changes in for example ENSO asymmetry in amplitude, duration, and transition from the 20th to the 21st century the model agreement is poor, trends are not significant and the variations mostly lie within the range of natural variability. Our findings also support the results from the studies by Zheng et al. (2018) and Maher et al. (2018) who did similar analyses but for ENSO amplitude and also attribute most inter-member variability to natural variability.

Our results suggest that the uncertainties might only be marginally reducible, since only the uncertainties due to model differences can be minimised but not the natural variability. This means that it is impossible to make reliable predictions of changes in ENSO frequency based on 120 years of model simulations. Although we used only a particular type of model (coupled climate models as represented in CMIP) we think that this result is general, since the main finding is that the natural variability is so large, and this is unlikely to change for more sophisticated models. Therefore, even if models that represent ENSO dynamics more faithfully may exhibit larger and/or more robust ENSO frequency trends, natural variability is still likely to dominate.

### Acronyms

**CMIP5** Coupled Model Intercomparison Project Phase 5

**CMIP6** Coupled Model Intercomparison Project Phase 6

**ENSO** El Niño Southern Oscillation

**EOF** empirical orthogonal function

**PC** principle component

**SST** sea surface temperature

### Acknowledgments

We thank the WorldClimate Research Programme's Working Group on Coupled Modelling who are responsible for CMIP6, for making the datasets used in this study publicly available. Special thanks to the modelling groups and institutes that responsible for the models listed in table 1. All CMIP6 data used in this work is made available by the DKRZ (Deutsches Klimarechenzentrum). We also want to send special thanks to the

259 Max-Planck Institute for Meteorology in Hamburg for providing the MPI-ESM-LR sim-  
260 ulations.

261 Thanks to Thorsten Mauritsen for the idea to look at the control runs. Thanks also  
262 go to Oliver Lemke for any kind of technical support.

263 With this study we contribute to the Center for Earth System Research and Sus-  
264 tainability (CEN) of Universität Hamburg. The work of Fiona Fix was supported by the  
265 Deutsche Forschungsgemeinschaft (DFG, German Research Foundation) under Germany's  
266 Excellence Strategy – EXC 2037 'CLICCS - Climate, Climatic Change, and Society' –  
267 Project Number: 390683824.

## 268 References

- 269 Bader, D. C., Leung, R., Taylor, M., & McCoy, R. B. (2019). *E3SM-Project*  
270 *E3SM1.0 model output prepared for CMIP6 CMIP*. Earth System Grid Fed-  
271 eration. Retrieved from <https://doi.org/10.22033/ESGF/CMIP6.2294> doi:  
272 10.22033/ESGF/CMIP6.2294
- 273 Bentsen, M., Olivière, D. J. L., Seland, y., Toniazzo, T., Gjermundsen, A., Graff, L. S.,  
274 ... Schulz, M. (2019). *NCC NorESM2-MM model output prepared for CMIP6*  
275 *CMIP*. Earth System Grid Federation. Retrieved from [https://doi.org/](https://doi.org/10.22033/ESGF/CMIP6.506)  
276 [10.22033/ESGF/CMIP6.506](https://doi.org/10.22033/ESGF/CMIP6.506) doi: 10.22033/ESGF/CMIP6.506
- 277 Berner, J., Christensen, H. M., & Sardeshmukh, P. D. (2020). Does ENSO Regu-  
278 larity Increase in a Warming Climate? *Journal of Climate*, *33*(4), 1247-1259.  
279 Retrieved from <https://doi.org/10.1175/JCLI-D-19-0545.1> doi: 10.1175/  
280 JCLI-D-19-0545.1
- 281 Bethke, I., Wang, Y., Counillon, F., Kimmritz, M., Fransner, F., Samuelsen, A., ...  
282 Keenlyside, N. (2019). *NCC NorCPM1 model output prepared for CMIP6*  
283 *CMIP*. Earth System Grid Federation. Retrieved from [https://doi.org/](https://doi.org/10.22033/ESGF/CMIP6.10843)  
284 [10.22033/ESGF/CMIP6.10843](https://doi.org/10.22033/ESGF/CMIP6.10843) doi: 10.22033/ESGF/CMIP6.10843
- 285 Boucher, O., Denvil, S., Levassasseur, G., Cozic, A., Caubel, A., Foujols, M.-A., ...  
286 Cheruy, F. (2018). *IPSL IPSL-CM6A-LR model output prepared for CMIP6*  
287 *CMIP*. Earth System Grid Federation. Retrieved from [https://doi.org/](https://doi.org/10.22033/ESGF/CMIP6.1534)  
288 [10.22033/ESGF/CMIP6.1534](https://doi.org/10.22033/ESGF/CMIP6.1534) doi: 10.22033/ESGF/CMIP6.1534
- 289 Cai, W., Borlace, S., Lengaigne, M., Rensch, P., Collins, M., Vecchi, G., ... Jin,  
290 F.-F. (2014). Increasing Frequency of Extreme El Nino Events due to  
291 Greenhouse Warming. *Nature Climate Change*, *4*, 111–116. Retrieved from  
292 <https://doi.org/10.1038/nclimate2100> doi: 10.1038/nclimate2100
- 293 Cai, W., Santoso, A., Wang, G., Yeh, S.-W., An, S.-I., Cobb, K. M., ... Wu,  
294 L. (2015). ENSO and greenhouse warming. *Nature Climate Change*, *5*,  
295 849-859. Retrieved from <https://doi.org/10.1038/nclimate2743> doi:  
296 10.1038/nclimate2743
- 297 Cai, W., Wang, G., Santoso, A., McPhaden, M., Wu, L., Jin, F.-F., ... Guil-  
298 yardi, E. (2015). Increased frequency of extreme La Niña events under  
299 greenhouse warming. *Nature Climate Change*, *5*, 132-137. Retrieved from  
300 <https://doi.org/10.1038/nclimate2492> doi: 10.1038/nclimate2492
- 301 Cao, J., & Wang, B. (2019). *NUIST NESMv3 model output prepared for CMIP6*  
302 *CMIP*. Earth System Grid Federation. Retrieved from [https://doi.org/10](https://doi.org/10.22033/ESGF/CMIP6.2021)  
303 [.22033/ESGF/CMIP6.2021](https://doi.org/10.22033/ESGF/CMIP6.2021) doi: 10.22033/ESGF/CMIP6.2021
- 304 Chen, C., Cane, M. A., Wittenberg, A. T., & Chen, D. (2017). ENSO in the CMIP5  
305 Simulations: Life Cycles, Diversity, and Responses to Climate Change. *Jour-  
306 nal of Climate*, *30*(2), 775 - 801. Retrieved from [https://journals.ametsoc](https://journals.ametsoc.org/view/journals/clim/30/2/jcli-d-15-0901.1.xml)  
307 [.org/view/journals/clim/30/2/jcli-d-15-0901.1.xml](https://journals.ametsoc.org/view/journals/clim/30/2/jcli-d-15-0901.1.xml) doi: 10.1175/JCLI  
308 -D-15-0901.1
- 309 Collins, M. (2000a). The el niño–southern oscillation in the second hadley centre  
310 coupled model and its response to greenhouse warming. *Journal of Climate*,

- 311 13(7), 1299 - 1312. Retrieved from [https://journals.ametsoc.org/view/journals/clim/13/7/1520-0442-2000-013\\_1299\\_tenos0\\_2.0.co-2.xml](https://journals.ametsoc.org/view/journals/clim/13/7/1520-0442-2000-013_1299_tenos0_2.0.co-2.xml) doi:  
312 10.1175/1520-0442(2000)013<1299:TENOSO>2.0.CO;2  
313
- 314 Collins, M. (2000b). Understanding uncertainties in the response of ENSO to green-  
315 house warming. *Geophysical Research Letters*, 27(21), 3509-3512. Retrieved  
316 from [https://agupubs.onlinelibrary.wiley.com/doi/abs/10.1029/](https://agupubs.onlinelibrary.wiley.com/doi/abs/10.1029/2000GL011747)  
317 [2000GL011747](https://doi.org/10.1029/2000GL011747) doi: <https://doi.org/10.1029/2000GL011747>
- 318 Danabasoglu, G. (2019a). *NCAR CESM2-FV2 model output prepared for CMIP6*  
319 *CMIP*. Earth System Grid Federation. Retrieved from [https://doi.org/10](https://doi.org/10.22033/ESGF/CMIP6.11281)  
320 [.22033/ESGF/CMIP6.11281](https://doi.org/10.22033/ESGF/CMIP6.11281) doi: 10.22033/ESGF/CMIP6.11281
- 321 Danabasoglu, G. (2019b). *NCAR CESM2 model output prepared for CMIP6 CMIP*.  
322 Earth System Grid Federation. Retrieved from [https://doi.org/10.22033/](https://doi.org/10.22033/ESGF/CMIP6.2185)  
323 [ESGF/CMIP6.2185](https://doi.org/10.22033/ESGF/CMIP6.2185) doi: 10.22033/ESGF/CMIP6.2185
- 324 Danabasoglu, G. (2019c). *NCAR CESM2-WACCM-FV2 model output prepared for*  
325 *CMIP6 CMIP*. Earth System Grid Federation. Retrieved from [https://doi](https://doi.org/10.22033/ESGF/CMIP6.11282)  
326 [.org/10.22033/ESGF/CMIP6.11282](https://doi.org/10.22033/ESGF/CMIP6.11282) doi: 10.22033/ESGF/CMIP6.11282
- 327 Danabasoglu, G. (2019d). *NCAR CESM2-WACCM model output prepared for*  
328 *CMIP6 CMIP*. Earth System Grid Federation. Retrieved from [https://](https://doi.org/10.22033/ESGF/CMIP6.10024)  
329 [doi.org/10.22033/ESGF/CMIP6.10024](https://doi.org/10.22033/ESGF/CMIP6.10024) doi: 10.22033/ESGF/CMIP6.10024
- 330 Deng, L., Yang, X., & Xie, Q. (2010). ENSO frequency change in coupled cli-  
331 mate models as response to the increasing CO<sub>2</sub> concentration. *Chinese Sci-*  
332 *ence Bulletin*, 55, 744-751. Retrieved from [https://doi.org/10.1007/](https://doi.org/10.1007/s11434-009-0491-x)  
333 [s11434-009-0491-x](https://doi.org/10.1007/s11434-009-0491-x) doi: 10.1007/s11434-009-0491-x
- 334 Dix, M., Bi, D., Dobrohotoff, P., Fiedler, R., Harman, I., Law, R., ... Yang, R.  
335 (2019). *CSIRO-ARCCSS ACCESS-CM2 model output prepared for CMIP6*  
336 *CMIP*. Earth System Grid Federation. Retrieved from [https://doi.org/](https://doi.org/10.22033/ESGF/CMIP6.2281)  
337 [10.22033/ESGF/CMIP6.2281](https://doi.org/10.22033/ESGF/CMIP6.2281) doi: 10.22033/ESGF/CMIP6.2281
- 338 Dommenges, D., Bayr, T., & Frauen, C. (2013). Analysis of the non-linearity in the  
339 pattern and time evolution of El Niño southern oscillation. *Climate Dynamics*,  
340 40, 2825-2847. Retrieved from [https://doi.org/10.1007/s00382-012-1475](https://doi.org/10.1007/s00382-012-1475-0)  
341 [-0](https://doi.org/10.1007/s00382-012-1475-0) doi: 10.1007/s00382-012-1475-0
- 342 EC-Earth Consortium. (2019). *EC-Earth-Consortium EC-Earth3 model output*  
343 *prepared for CMIP6 CMIP*. Earth System Grid Federation. Retrieved from  
344 <https://doi.org/10.22033/ESGF/CMIP6.181> doi: 10.22033/ESGF/CMIP6  
345 .181
- 346 Eyring, V., Bony, S., Meehl, G. A., Senior, C. A., Stevens, B., Stouffer, R. J., &  
347 Taylor, K. E. (2016). Overview of the Coupled Model Intercomparison Project  
348 Phase 6 (CMIP6) experimental design and organization. *Geoscientific Model*  
349 *Development*, 9(5), 1937-1958. Retrieved from [https://gmd.copernicus](https://gmd.copernicus.org/articles/9/1937/2016/)  
350 [.org/articles/9/1937/2016/](https://gmd.copernicus.org/articles/9/1937/2016/) doi: 10.5194/gmd-9-1937-2016
- 351 Giorgetta, M. A., Jungclaus, J., Reick, C. H., Legutke, S., Bader, J., Böttinger, M.,  
352 ... Stevens, B. (2013). Climate and carbon cycle changes from 1850 to 2100 in  
353 MPI-ESM simulations for the Coupled Model Intercomparison Project phase 5.  
354 *Journal of Advances in Modeling Earth Systems*, 5(3), 572-597. Retrieved from  
355 <https://agupubs.onlinelibrary.wiley.com/doi/abs/10.1002/jame.20038>  
356 doi: 10.1002/jame.20038
- 357 Guilyardi, E. (2006). El Niño-mean state-seasonal cycle interactions in a multi-  
358 model ensemble. *Climate Dynamics*, 26, 329-348. Retrieved from [https://doi](https://doi.org/10.1007/s00382-005-0084-6)  
359 [.org/10.1007/s00382-005-0084-6](https://doi.org/10.1007/s00382-005-0084-6) doi: 10.1007/s00382-005-0084-6
- 360 Guo, H., John, J. G., Blanton, C., McHugh, C., Nikonov, S., Radhakrishnan, A.,  
361 ... Zhang, R. (2018). *NOAA-GFDL GFDL-CM4 model output*. Earth Sys-  
362 tem Grid Federation. Retrieved from [https://doi.org/10.22033/ESGF/](https://doi.org/10.22033/ESGF/CMIP6.1402)  
363 [CMIP6.1402](https://doi.org/10.22033/ESGF/CMIP6.1402) doi: 10.22033/ESGF/CMIP6.1402
- 364 Hajima, T., Abe, M., Arakawa, O., Suzuki, T., Komuro, Y., Ogura, T., ... Tachiiri,  
365 K. (2019). *MIROC MIROC-ES2L model output prepared for CMIP6 CMIP*.

- 366 Earth System Grid Federation. Retrieved from [https://doi.org/10.22033/](https://doi.org/10.22033/ESGF/CMIP6.902)  
 367 [ESGF/CMIP6.902](https://doi.org/10.22033/ESGF/CMIP6.902) doi: 10.22033/ESGF/CMIP6.902
- 368 Huang, W. (2019). *THU CIESM model output prepared for CMIP6 CMIP*. Earth  
 369 System Grid Federation. Retrieved from [https://doi.org/10.22033/ESGF/](https://doi.org/10.22033/ESGF/CMIP6.1352)  
 370 [CMIP6.1352](https://doi.org/10.22033/ESGF/CMIP6.1352) doi: 10.22033/ESGF/CMIP6.1352
- 371 Jungclaus, J., Bittner, M., Wieners, K.-H., Wachsmann, F., Schupfner, M., Legutke,  
 372 S., ... Roeckner, E. (2019). *MPI-M MPIESM1.2-HR model output prepared*  
 373 *for CMIP6 CMIP*. Earth System Grid Federation. Retrieved from [https://](https://doi.org/10.22033/ESGF/CMIP6.741)  
 374 [doi.org/10.22033/ESGF/CMIP6.741](https://doi.org/10.22033/ESGF/CMIP6.741) doi: 10.22033/ESGF/CMIP6.741
- 375 Maher, N., Matei, D., Milinski, S., & Marotzke, J. (2018). ENSO Change in  
 376 Climate Projections: Forced Response or Internal Variability? *Geophys-*  
 377 *ical Research Letters*, 45(20), 11,390-11,398. Retrieved from [https://](https://agupubs.onlinelibrary.wiley.com/doi/abs/10.1029/2018GL079764)  
 378 [agupubs.onlinelibrary.wiley.com/doi/abs/10.1029/2018GL079764](https://agupubs.onlinelibrary.wiley.com/doi/abs/10.1029/2018GL079764) doi:  
 379 <https://doi.org/10.1029/2018GL079764>
- 380 Merryfield, W. J. (2006). Changes to ENSO under CO2 Doubling in a Multimodel  
 381 Ensemble. *Journal of Climate*, 19(16), 4009 - 4027. Retrieved from [https://](https://journals.ametsoc.org/view/journals/clim/19/16/jcli3834.1.xml)  
 382 [journals.ametsoc.org/view/journals/clim/19/16/jcli3834.1.xml](https://journals.ametsoc.org/view/journals/clim/19/16/jcli3834.1.xml) doi:  
 383 [10.1175/JCLI3834.1](https://doi.org/10.1175/JCLI3834.1)
- 384 NASA/GISS. (2018a). *NASA-GISS GISS-E2.1G model output prepared for CMIP6*  
 385 *CMIP*. Earth System Grid Federation. Retrieved from [https://doi.org/10](https://doi.org/10.22033/ESGF/CMIP6.1400)  
 386 [.22033/ESGF/CMIP6.1400](https://doi.org/10.22033/ESGF/CMIP6.1400) doi: 10.22033/ESGF/CMIP6.1400
- 387 NASA/GISS. (2018b). *NASA-GISS GISS-E2.1H model output prepared for CMIP6*  
 388 *CMIP*. Earth System Grid Federation. Retrieved from [https://doi.org/10](https://doi.org/10.22033/ESGF/CMIP6.1421)  
 389 [.22033/ESGF/CMIP6.1421](https://doi.org/10.22033/ESGF/CMIP6.1421) doi: 10.22033/ESGF/CMIP6.1421
- 390 NASA/GISS. (2019). *NASA-GISS GISS-E2-2-G model output prepared for CMIP6*  
 391 *CMIP*. Earth System Grid Federation. Retrieved from [https://doi.org/10](https://doi.org/10.22033/ESGF/CMIP6.2081)  
 392 [.22033/ESGF/CMIP6.2081](https://doi.org/10.22033/ESGF/CMIP6.2081) doi: 10.22033/ESGF/CMIP6.2081
- 393 Neubauer, D., Ferrachat, S., Siegenthaler-Le Drian, C., Stoll, J., Folini, D. S.,  
 394 Tegen, I., ... Lohmann, U. (2019). *HAMMOZ-Consortium MPI-ESM1.2-*  
 395 *HAM model output prepared for CMIP6 CMIP*. Earth System Grid Federa-  
 396 tion. Retrieved from <https://doi.org/10.22033/ESGF/CMIP6.1622> doi:  
 397 [10.22033/ESGF/CMIP6.1622](https://doi.org/10.22033/ESGF/CMIP6.1622)
- 398 NOAA Climate Prediction Center, National Weather Service. (2020a). *Cold &*  
 399 *Warm Episodes by Season*. Retrieved from [https://origin.cpc.ncep.noaa](https://origin.cpc.ncep.noaa.gov/products/analysis_monitoring/ensostuff/ONI.v5.php)  
 400 [.gov/products/analysis\\_monitoring/ensostuff/ONI.v5.php](https://origin.cpc.ncep.noaa.gov/products/analysis_monitoring/ensostuff/ONI.v5.php) (Online, last  
 401 accessed 22-March-2021)
- 402 NOAA Climate Prediction Center, National Weather Service. (2020b). *Descrip-*  
 403 *tion of Changes to Ocean Niño Index (ONI)*. Retrieved from [https://](https://origin.cpc.ncep.noaa.gov/products/analysis_monitoring/ensostuff/ONI_change.shtml)  
 404 [origin.cpc.ncep.noaa.gov/products/analysis\\_monitoring/ensostuff/](https://origin.cpc.ncep.noaa.gov/products/analysis_monitoring/ensostuff/ONI_change.shtml)  
 405 [ONI\\_change.shtml](https://origin.cpc.ncep.noaa.gov/products/analysis_monitoring/ensostuff/ONI_change.shtml) (Online, last accessed 22-March-2021)
- 406 Park, S., & Shin, J. (2019). *SNU SAM0-UNICON model output prepared for CMIP6*  
 407 *CMIP*. Earth System Grid Federation. Retrieved from [https://doi.org/10](https://doi.org/10.22033/ESGF/CMIP6.1489)  
 408 [.22033/ESGF/CMIP6.1489](https://doi.org/10.22033/ESGF/CMIP6.1489) doi: 10.22033/ESGF/CMIP6.1489
- 409 Penland, C., & Sardeshmukh, P. D. (1995). The Optimal Growth of Tropical Sea  
 410 Surface Temperature Anomalies. *Journal of Climate*, 8(8), 1999-2024. Re-  
 411 trieved from [https://doi.org/10.1175/1520-0442\(1995\)008<1999:TOGOTS>](https://doi.org/10.1175/1520-0442(1995)008<1999:TOGOTS>2.0.CO;2)  
 412 [2.0.CO;2](https://doi.org/10.1175/1520-0442(1995)008<1999:TOGOTS>2.0.CO;2) doi: 10.1175/1520-0442(1995)008<1999:TOGOTS>2.0.CO;2
- 413 Plesca, E., Grützun, V., & Buehler, S. A. (2018). How robust is the weakening  
 414 of the pacific walker circulation in cmip5 idealized transient climate sim-  
 415 ulations? *Journal of Climate*, 31(1), 81 - 97. Retrieved from [https://](https://journals.ametsoc.org/view/journals/clim/31/1/jcli-d-17-0151.1.xml)  
 416 [journals.ametsoc.org/view/journals/clim/31/1/jcli-d-17-0151.1.xml](https://journals.ametsoc.org/view/journals/clim/31/1/jcli-d-17-0151.1.xml)  
 417 doi: 10.1175/JCLI-D-17-0151.1
- 418 Ridley, J., Menary, M., Kuhlbrodt, T., Andrews, M., & Andrews, T. (2018). *MOHC*  
 419 *HadGEM3-GC31-LL model output prepared for CMIP6 CMIP*. Earth Sys-  
 420 tem Grid Federation. Retrieved from <https://doi.org/10.22033/ESGF/>

- 421 CMIP6.419 doi: 10.22033/ESGF/CMIP6.419
- 422 Rong, X. (2019). *CAMS CAMS-CSM1.0 model output prepared for CMIP6 CMIP.*  
 423 Earth System Grid Federation. Retrieved from [https://doi.org/10.22033/](https://doi.org/10.22033/ESGF/CMIP6.1399)  
 424 [ESGF/CMIP6.1399](https://doi.org/10.22033/ESGF/CMIP6.1399) doi: 10.22033/ESGF/CMIP6.1399
- 425 Seferian, R. (2018). *CNRM-CERFACS CNRM-ESM2-1 model output prepared for*  
 426 *CMIP6 CMIP.* Earth System Grid Federation. Retrieved from [https://doi](https://doi.org/10.22033/ESGF/CMIP6.1391)  
 427 [.org/10.22033/ESGF/CMIP6.1391](https://doi.org/10.22033/ESGF/CMIP6.1391) doi: 10.22033/ESGF/CMIP6.1391
- 428 Seland, y., Bentsen, M., Olivie, D. J. L., Toniazzo, T., Gjermundsen, A., Graff, L. S.,  
 429 ... Schulz, M. (2019). *NCC NorESM2-LM model output prepared for CMIP6*  
 430 *CMIP.* Earth System Grid Federation. Retrieved from [https://doi.org/](https://doi.org/10.22033/ESGF/CMIP6.502)  
 431 [10.22033/ESGF/CMIP6.502](https://doi.org/10.22033/ESGF/CMIP6.502) doi: 10.22033/ESGF/CMIP6.502
- 432 Semmler, T., Danilov, S., Rackow, T., Sidorenko, D., Barbi, D., Hegewald, J., ...  
 433 Jung, T. (2018). *AWI AWI-CM1.1MR model output prepared for CMIP6*  
 434 *CMIP.* Earth System Grid Federation. Retrieved from [https://doi.org/](https://doi.org/10.22033/ESGF/CMIP6.359)  
 435 [10.22033/ESGF/CMIP6.359](https://doi.org/10.22033/ESGF/CMIP6.359) doi: 10.22033/ESGF/CMIP6.359
- 436 Song, Z., Qiao, F., Bao, Y., Shu, Q., Song, Y., & Yang, X. (2019). *FIO-QLNM FIO-*  
 437 *ESM2.0 model output prepared for CMIP6 CMIP.* Earth System Grid Federa-  
 438 tion. Retrieved from <https://doi.org/10.22033/ESGF/CMIP6.9047> doi: 10.  
 439 [.22033/ESGF/CMIP6.9047](https://doi.org/10.22033/ESGF/CMIP6.9047)
- 440 Stevens, B., Giorgetta, M., Esch, M., Mauritsen, T., Crueger, T., Rast, S., ...  
 441 Roeckner, E. (2013). Atmospheric component of the MPI-M Earth System  
 442 Model: ECHAM6. *Journal of Advances in Modeling Earth Systems*, 5(2),  
 443 146-172. Retrieved from [https://agupubs.onlinelibrary.wiley.com/doi/](https://agupubs.onlinelibrary.wiley.com/doi/abs/10.1002/jame.20015)  
 444 [abs/10.1002/jame.20015](https://agupubs.onlinelibrary.wiley.com/doi/abs/10.1002/jame.20015) doi: 10.1002/jame.20015
- 445 Stouffer, R. (2019). *U of Arizona MCM-UA-1-0 model output prepared for CMIP6*  
 446 *CMIP.* Earth System Grid Federation. Retrieved from [https://doi.org/10](https://doi.org/10.22033/ESGF/CMIP6.2421)  
 447 [.22033/ESGF/CMIP6.2421](https://doi.org/10.22033/ESGF/CMIP6.2421) doi: 10.22033/ESGF/CMIP6.2421
- 448 Swart, N. C., Cole, J. N., Kharin, V. V., Lazare, M., Scinocca, J. F., Gillett, N. P.,  
 449 ... Sigmond, M. (2019). *CCCma CanESM5 model output prepared for CMIP6*  
 450 *CMIP.* Earth System Grid Federation. Retrieved from [https://doi.org/](https://doi.org/10.22033/ESGF/CMIP6.1303)  
 451 [10.22033/ESGF/CMIP6.1303](https://doi.org/10.22033/ESGF/CMIP6.1303) doi: 10.22033/ESGF/CMIP6.1303
- 452 Tang, Y., Rumbold, S., Ellis, R., Kelley, D., Mulcahy, J., Sellar, A., ... Jones, C.  
 453 (2019). *MOHC UKESM1.0-LL model output prepared for CMIP6 CMIP.*  
 454 Earth System Grid Federation. Retrieved from [https://doi.org/10.22033/](https://doi.org/10.22033/ESGF/CMIP6.1569)  
 455 [ESGF/CMIP6.1569](https://doi.org/10.22033/ESGF/CMIP6.1569) doi: 10.22033/ESGF/CMIP6.1569
- 456 Tatebe, H., & Watanabe, M. (2018). *MIROC MIROC6 model output prepared for*  
 457 *CMIP6 CMIP.* Earth System Grid Federation. Retrieved from [https://doi](https://doi.org/10.22033/ESGF/CMIP6.881)  
 458 [.org/10.22033/ESGF/CMIP6.881](https://doi.org/10.22033/ESGF/CMIP6.881) doi: 10.22033/ESGF/CMIP6.881
- 459 Timmermann, A. (2001). Changes of enso stability due to greenhouse warming.  
 460 *Geophysical Research Letters*, 28(10), 2061-2064. Retrieved from [https://](https://agupubs.onlinelibrary.wiley.com/doi/abs/10.1029/2001GL012879)  
 461 [agupubs.onlinelibrary.wiley.com/doi/abs/10.1029/2001GL012879](https://agupubs.onlinelibrary.wiley.com/doi/abs/10.1029/2001GL012879) doi:  
 462 <https://doi.org/10.1029/2001GL012879>
- 463 Timmermann, A., Oberhuber, J., Bacher, A., Esch, M., Latif, M., & Roeck-  
 464 ner, E. (1999). Increased El Niño frequency in a climate model forced  
 465 by future greenhouse warming. *Nature*, 398, 694-697. Retrieved from  
 466 <https://doi.org/10.1038/19505> doi: 10.1038/19505
- 467 Voldoire, A. (2018). *CNRM-CERFACS CNRM-CM6-1 model output prepared for*  
 468 *CMIP6 CMIP.* Earth System Grid Federation. Retrieved from [https://doi](https://doi.org/10.22033/ESGF/CMIP6.1375)  
 469 [.org/10.22033/ESGF/CMIP6.1375](https://doi.org/10.22033/ESGF/CMIP6.1375) doi: 10.22033/ESGF/CMIP6.1375
- 470 Voldoire, A. (2019). *CNRM-CERFACS CNRM-CM6-1-HR model output prepared for*  
 471 *CMIP6 CMIP.* Earth System Grid Federation. Retrieved from [https://doi](https://doi.org/10.22033/ESGF/CMIP6.1385)  
 472 [.org/10.22033/ESGF/CMIP6.1385](https://doi.org/10.22033/ESGF/CMIP6.1385) doi: 10.22033/ESGF/CMIP6.1385
- 473 Volodin, E., Mortikov, E., Gritsun, A., Lykossov, V., Galin, V., Diansky, N., ...  
 474 Emelina, S. (2019a). *INM INM-CM4-8 model output prepared for CMIP6*  
 475 *CMIP.* Earth System Grid Federation. Retrieved from <https://doi.org/>

- 476 10.22033/ESGF/CMIP6.1422 doi: 10.22033/ESGF/CMIP6.1422  
 477 Volodin, E., Mortikov, E., Gritsun, A., Lykossov, V., Galin, V., Diansky, N., ...  
 478 Emelina, S. (2019b). *INM INM-CM5-0 model output prepared for CMIP6*  
 479 *CMIP*. Earth System Grid Federation. Retrieved from [https://doi.org/](https://doi.org/10.22033/ESGF/CMIP6.1423)  
 480 10.22033/ESGF/CMIP6.1423 doi: 10.22033/ESGF/CMIP6.1423  
 481 Wang, G., Cai, W., Gan, B., Wu, L., Santoso, A., Lin, X., ... McPhaden, M. J.  
 482 (2017). Continued increase of extreme El Niño frequency long after 1.5 °C  
 483 warming stabilization. *Nature Climate Change*, 7(8), 568-572. Retrieved  
 484 from <https://ui.adsabs.harvard.edu/abs/2017NatCC...7..568W> doi:  
 485 10.1038/nclimate3351  
 486 Wieners, K.-H., Giorgetta, M., Jungclaus, J., Reick, C., Esch, M., Bittner, M., ...  
 487 Roeckner, E. (2019). *MPI-M MPIESM1.2-LR model output prepared for*  
 488 *CMIP6 CMIP*. Earth System Grid Federation. Retrieved from [https://](https://doi.org/10.22033/ESGF/CMIP6.742)  
 489 [doi.org/10.22033/ESGF/CMIP6.742](https://doi.org/10.22033/ESGF/CMIP6.742) doi: 10.22033/ESGF/CMIP6.742  
 490 Xin, X., Zhang, J., Zhang, F., Wu, T., Shi, X., Li, J., ... Wei, M. (2018). *BCC*  
 491 *BCC-CSM2MR model output prepared for CMIP6 CMIP*. Earth System Grid  
 492 Federation. Retrieved from <https://doi.org/10.22033/ESGF/CMIP6.1725>  
 493 doi: 10.22033/ESGF/CMIP6.1725  
 494 Xu, K., Tam, C.-Y., Zhu, C., Liu, B., & Wang, W. (2017). CMIP5 Projec-  
 495 tions of Two Types of El Niño and Their Related Tropical Precipitation  
 496 in the Twenty-First Century. *Journal of Climate*, 30(3), 849 - 864. Re-  
 497 trieved from [https://journals.ametsoc.org/view/journals/clim/30/3/](https://journals.ametsoc.org/view/journals/clim/30/3/jcli-d-16-0413.1.xml)  
 498 [jcli-d-16-0413.1.xml](https://journals.ametsoc.org/view/journals/clim/30/3/jcli-d-16-0413.1.xml) doi: 10.1175/JCLI-D-16-0413.1  
 499 Yang, H., Zhang, Q., Zhong, Y., Vavrus, S., & Liu, Z. (2005). How does extratrop-  
 500 ical warming affect ENSO? *Geophysical Research Letters*, 32(1). Retrieved  
 501 from [https://agupubs.onlinelibrary.wiley.com/doi/abs/10.1029/](https://agupubs.onlinelibrary.wiley.com/doi/abs/10.1029/2004GL021624)  
 502 [2004GL021624](https://agupubs.onlinelibrary.wiley.com/doi/abs/10.1029/2004GL021624) doi: <https://doi.org/10.1029/2004GL021624>  
 503 Yukimoto, S., Koshiro, T., Kawai, H., Oshima, N., Yoshida, K., Urakawa, S., ...  
 504 Adachi, Y. (2019). *MRI MRI-ESM2.0 model output prepared for CMIP6*  
 505 *CMIP*. Earth System Grid Federation. Retrieved from [https://doi.org/](https://doi.org/10.22033/ESGF/CMIP6.621)  
 506 10.22033/ESGF/CMIP6.621 doi: 10.22033/ESGF/CMIP6.621  
 507 Zelle, H., van Oldenborgh, G. J., Burgers, G., & Dijkstra, H. (2005). El Niño and  
 508 Greenhouse Warming: Results from Ensemble Simulations with the NCAR  
 509 CCSM. *Journal of Climate*, 18(22), 4669 - 4683. Retrieved from [https://](https://journals.ametsoc.org/view/journals/clim/18/22/jcli3574.1.xml)  
 510 [journals.ametsoc.org/view/journals/clim/18/22/jcli3574.1.xml](https://journals.ametsoc.org/view/journals/clim/18/22/jcli3574.1.xml) doi:  
 511 10.1175/JCLI3574.1  
 512 Zhang, J., Wu, T., Shi, X., Zhang, F., Li, J., Chu, M., ... Wei, M. (2018). *BCC*  
 513 *BCC-ESM1 model output prepared for CMIP6 CMIP*. Earth System Grid Fed-  
 514 eration. Retrieved from <https://doi.org/10.22033/ESGF/CMIP6.1734> doi:  
 515 10.22033/ESGF/CMIP6.1734  
 516 Zheng, X.-T., Hui, C., & Yeh, S.-W. (2018). Response of ENSO amplitude to global  
 517 warming in CESM large ensemble: uncertainty due to internal variability.  
 518 *Climate Dynamics*, 50(11), 4019-4035. Retrieved from [https://doi.org/](https://doi.org/10.1007/s00382-017-3859-7)  
 519 [10.1007/s00382-017-3859-7](https://doi.org/10.1007/s00382-017-3859-7) doi: 10.1007/s00382-017-3859-7  
 520 Ziehn, T., Chamberlain, M., Lenton, A., Law, R., Bodman, R., Dix, M., ... Druken,  
 521 K. (2019). *CSIRO ACCESS-ESM1.5 model output prepared for CMIP6 CMIP*.  
 522 Earth System Grid Federation. Retrieved from [https://doi.org/10.22033/](https://doi.org/10.22033/ESGF/CMIP6.2288)  
 523 [ESGF/CMIP6.2288](https://doi.org/10.22033/ESGF/CMIP6.2288) doi: 10.22033/ESGF/CMIP6.2288